Identification of functional cooperative mutations of *SETD2* in human acute leukemia

Xiaofan Zhu[1,10], **Fuhong He**[2,10], **Huimin Zeng**[1,10], **Shaoping Ling**[2,10], **Aili Chen**[2,3,4,5,10], **Yaqin Wang**[1], **Xiaomei Yan**[3,4], **Wei Wei**[1], **Yakun Pang**[1], **Hui Cheng**[1], **Chunlan Hua**[1], **Yue Zhang**[1,3,4], **Xuejing Yang**[2,5], **Xin Lu**[2,5], **Lihua Cao**[2], **Lingtong Hao**[2], **Lili Dong**[2], **Wei Zou**[2], **Jun Wu**[2], **Xia Li**[2,5], **Si Zheng**[2,5], **Jin Yan**[2], **Jing Zhou**[2], **Lixia Zhang**[2,5], **Shuangli Mi**[2], **Xiaojuan Wang**[1], **Li Zhang**[1], **Yao Zou**[1], **Yumei Chen**[1], **Zhe Geng**[6], **Jianmin Wang**[7], **Jianfeng Zhou**[6], **Xin Liu**[8,9], **Jianxiang Wang**[1], **Weiping Yuan**[1], **Gang Huang**[3,4], **Tao Cheng**[1], and **Qian-fei Wang**[2]

[1]State Key Laboratory of Experimental Hematology, Institute of Hematology and Blood Diseases Hospital and Center for Stem Cell Medicine, Chinese Academy of Medical Sciences and Peking Union Medical College, Tianjin, China

[2]Laboratory of Genome Variations and Precision Bio-Medicine, Beijing Institute of Genomics, Chinese Academy of Sciences, Beijing, China

[3]Division of Pathology, Cincinnati Children's Hospital Medical Center, Cincinnati, Ohio, USA

[4]Divisions of Experimental Hematology and Cancer Biology, Cincinnati Children's Hospital, Cincinnati, Ohio, USA

[5]University of Chinese Academy of Sciences, Beijing, China

[6]Department of Hematology, TongJi Hospital, TongJi Medical College, HuaZhong University of Science and Technology, Wuhan, Hubei, China

[7]Department of Hematology, Changhai Hospital, Second Military Medical University, Shanghai, China

[8]Mary Ann and J. Milburn Smith Child Health Research Program, Ann and Robert H. Lurie Children's Hospital of Chicago Research Center, Chicago, Illinois, USA

[9]Department of Pediatrics, Northwestern University Feinberg School of Medicine, Chicago, Illinois, USA

Abstract

Acute leukemia characterized by chromosomal rearrangements requires additional molecular disruptions to develop into full-blown malignancy[1,2], yet the cooperative mechanisms remain elusive. Using whole-genome sequencing of a pair of monozygotic twins discordant for *MLL* (also called *KMT2A*) gene-rearranged leukemia, we identified a transforming *MLL-NRIP3* fusion gene[3] and biallelic mutations in *SETD2* (encoding a histone H3K36 methyltransferase)[4]. Moreover, loss-of-function point mutations in *SETD2* were recurrent (6.2%) in 241 patients with acute leukemia and were associated with multiple major chromosomal aberrations. We observed a global loss of H3K36 trimethylation (H3K36me3) in leukemic blasts with mutations in *SETD2*. In the presence of a genetic lesion, downregulation of *SETD2* contributed to both initiation and progression during leukemia development by promoting the self-renewal potential of leukemia stem cells. Therefore, our study provides compelling evidence for *SETD2* as a new tumor suppressor. Disruption of the SETD2-H3K36me3 pathway is a distinct epigenetic mechanism for leukemia development.

Chromosomal translocations occur in more than 50% of human leukemias and lymphomas[5,6] and are increasingly being observed in solid tumors[7]. However, chromosomal translocation alone may not be sufficient to drive full-blown disease, even in pediatric leukemias[8,9]. To define cooperating genetic and epigenetic abnormalities that are associated with primary chromosomal translocations during the development of leukemia, we focused on a 3-year-old female monozygotic twin pair that is discordant for *MLL*-associated acute myeloid leukemia (AML) and has been morphologically classified as FAB-M5 (Supplementary Figs. 1 and 2 and Supplementary Note). FISH analysis indicated chromosomal translocation disrupting *MLL* in the patient with leukemia but not her twin sister (Supplementary Fig. 1). To characterize the unknown *MLL* fusion gene that resulted from the chromosomal rearrangement and detect all potential cooperative somatic genomic changes, we obtained 55× and 62× whole-genome sequencing (WGS) data covering 98.48% and 98.46% of the genomes of CD56^{+}CD64^{+} leukemia cells from the patient and peripheral blood mononuclear cells (PBMCs) from her healthy twin sister, respectively (Supplementary Table 1). With PBMCs from the healthy twin as a germline and normal tissue control, we revealed an intrachromosomal translocation that gave rise to the *MLL-NRIP3* fusion gene[3] in the twin with leukemia (Fig. 1a,b and Supplementary Figs. 3 and 4). Retrovirus-mediated ectopic expression of *MLL-NRIP3* in mouse hematopoietic cells was able to induce the same type of myeloid leukemia as that of the patient in a mouse transplant model (Fig. 1c,d and Supplementary Fig. 5). The median onset of the AML was 46.5 days (Fig. 1c), suggesting additional cooperative events in the development of induced leukemia.

In searching for potential cooperative somatic genomic alterations in the twin with leukemia (Fig. 1a, Supplementary Table 2 and Supplementary Figs. 3, 4, 6 and 7), we identified two non-synonymous point mutations in *SETD2* located in chromosome 3p (Supplementary Table 2), which encodes the only histone-modifying enzyme that is responsible for catalyzing H3K36me3 (ref. 10). Analysis of sequencing reads and further genotyping using Sequenom assay showed an approximate 50% allele frequency for each of the two mutations

(Supplementary Fig. 8), suggesting that these mutations are present in almost all of the leukemic cells. Methylation of H3K36 and H3K79 are the two major histone modifications that are involved in transcriptional elongation[11]. Given the previously documented role of MLL fusion protein–mediated H3K79 methylation in leukemogenesis[1], it was of great interest for us to explore whether a distinct epigenetic pathway represented by SETD2-H3K36 could be a cooperative event in the development of *MLL*-rearranged leukemia. Therefore, we focused all subsequent studies on the role of *SETD2* and its underlying mechanism in the development of leukemia.

To examine the prevalence of *SETD2* mutations in a general population of patients with leukemia, we next used PCR to amplify all 21 exons of *SETD2* and carried out Sanger sequencing on 134 AML and 107 acute lymphoblastic leukemia (ALL) samples (Supplementary Tables 3–6). We identified 19 somatic *SETD2* mutations in 15 patients (Fig. 2 and Table 1). We observed a higher frequency of *SETD2* mutations in *MLL*-rearranged patients with leukemia (22.2%, 6 out of 27) compared to patients with leukemia that did not have *MLL* rearrangements (4.6%, 8 out of 173) in the patient cohort ($P = 0.005$; Fig. 2 and Table 1). Notably, *SETD2* mutation is not unique to *MLL*-rearranged leukemia, as the *SETD2*-mutated patients also harbored a number of other known genetic aberrations, including *AML1* (also called *RUNX1*)-*ETO* (also called *RUNX1T1*) or mutations in *CEBPA* or *NPM1* (Table 1 and Supplementary Tables 3–6). Specifically, a majority of these patients with mutated *SETD2* (86.7%, 13 out of 15) had one additional major genetic aberration. Thus, these results demonstrate that *SETD2* mutations are recurrent in acute human leukemia and are associated with chromosomal abnormalities that are known to be driver mutations in leukemogenesis.

The mutation spectrum may imply the functional role of an affected gene acting as a tumor suppressor or oncogene in leukemia development[12]. We found that 8 of the total 19 *SETD2* mutations (42.1%) identified in 241 patients with acute leukemia were either nonsense or frameshift mutations that truncate a portion of the C terminus domain of SETD2 (Fig. 2a and Supplementary Table 3). In addition, 26.7% (4 out of 15) of the *SETD2*-mutated patients carried two mutations on *SETD2* (Table 1 and Supplementary Table 3). cDNA or DNA clone sequencing confirmed that each of the two mutations occurs on separate alleles of *SETD2* in individual patients, indicating a biallelic nature (Supplementary Table 3). These data are consistent with the notion of truncating mutations and/or multiple hits on the same gene, which are common mechanisms for inactivating the normal function of tumor-suppressor genes (Supplementary Fig. 9). Considering the loss-of-function feature of the *SETD2* mutations identified, we further explored whether additional genetic and epigenetic mechanisms operate to inactivate *SETD2* in acute leukemia (Supplementary Figs. 10 and 11). We found no evidence of *SETD2* gene deletion in our cohort of 241 patients with acute leukemia by Sequenom genotyping across chromosome 3 (Supplementary Fig. 10a). Using an established genomic analysis method[13,14], we detected large genomic deletions encompassing *SETD2* in patients with *MLL* fusion, as well as patients with *TEL* (also called *ETV6*)-*AML1* or *BCR-ABL*, but at a very low frequency (0.6%) (Supplementary Table 7 and Supplementary Fig. 11). This finding is in sharp contrast to the frequent (>80%) large deletions in *SETD2* in patients with clear cell renal cell carcinoma (ccRCC) detected by the

same genomic analysis (Supplementary Fig. 12) and by SNP array data[15,16] (Fig. 2b). In addition to genetic mutations, we detected downregulated mRNA expression of *SETD2* in patients with lymphoma and a subset of patients with leukemia at an ~9.0% frequency using expression data deposited in the Oncomine data set[17] (Supplementary Fig. 10b,c). However, downregulation of *SETD2* is unlikely due to epigenetic silencing, as we found no hypermethylation of *SETD2* promoter DNA in 194 AMLs from the DNA methylation data set derived from The Cancer Genome Atlas project[2] (TCGA; Supplementary Fig. 10d,e). Together these analyses strongly indicate that *SETD2* inactivation occurs primarily through point mutation and downregulation of gene expression in hematologic malignancies.

We further examined protein structural alterations of SETD2 and the associated histone methylation of H3K36 in *SETD2*-mutated patients. The majority (seven out of eight) of the truncating mutations in the patients resulted in loss of the C terminus SRI domain (Fig. 2a), which is responsible for the recruitment of SETD2 to its target gene locus through binding to the phosphor-C-terminal repeat domain (PCTD) of elongating RNA polymerase II (Pol II)[18]. Notably, in addition to a truncating mutation (NM_014159.6, c.6973C>T, p.Gln2325*; Supplementary Tables 2 and 3), the missense mutation (NM_014159.6, c.7515T>A, p.Phe2505Leu; Supplementary Tables 2 and 3) affecting the second allele of *SETD2* in the twin with leukemia mapped to the surface of the SRI domain (Fig. 3a) and corresponds to a key residue that is critical for the PCTD binding of SETD2 (ref. 18). It has been shown previously that the p.Phe2505Leu alteration blocks the binding of SETD2 to the PCTD of RNA Pol II at the target gene locus[18]. Consistent with published data[19,20], we observed a global decrease of H3K36me3 in CD56+CD64+ leukemia cells of the twin with *MLL*-rearranged leukemia but not in the CD56−CD64− non-leukemic cells from the same patient (Fig. 3b). Notably, additional patients with AML or ALL carrying *SETD2* mutations exhibited decreased levels of global H3K36me3, with the most substantial changes observed in patients with biallelic truncating mutations (Fig. 3c,d). Therefore, loss-of-function mutations of *SETD2* may impair the chromatin recruitment of SETD2 mediated by the SRI domain, which in turn contributes to the global loss of H3K36me3.

To test the functional importance of loss of function of *SETD2* in the development of myeloid leukemias characterized by either *MLL* translocation or additional genetic aberrations identified in patients, we employed bone marrow transplantation (BMT), as well as colony-forming cell and liquid culture assays, to demonstrate the transforming effects of *Setd2* knockdown *in vivo* and *in vitro*, respectively[21]. To determine the role of *SETD2* in disease initiation, we used several established pre-leukemia knock-in mouse models, including the *Mll-Af9* (also called *Mllt3*), *Mll*-PTD (partial tandem duplication) and *Aml1-Eto*, in which additional mutations are required to develop fullblown AML[22–26]. We compared the effects of *Setd2* knockdown in hematopoietic stem and progenitor cells (HSPCs) derived from wild-type or knock-in mice. Transfection of *Setd2* shRNA led to decreased levels of *Setd2* expression and H3K36me3, whereas H3K79me2 and H3K27me3 were minimally affected in the *Mll-Af9* knock-in cells (Fig. 4a and Supplementary Fig. 13). Consequently, *Setd2* knockdown resulted in a significantly higher yield of total colonies in the multiple rounds of plating for *Mll-Af9*, *Mll*-PTD and *Aml1-Eto* knock-in HSPCs (Fig. 4b). Consistently, *Setd2* knockdown equipped these pre-leukemic cells to gain a significant

growth advantage over serial passaging compared to control shRNA–treated cells in liquid culture (Fig. 4c). In contrast, colony-forming cell assays showed that knockdown of *Setd2* did not have a significant effect on wild-type HSPCs (Supplementary Fig. 14), suggesting an insufficient effect of Setd2 alteration alone on normal hematopoietic cell growth.

We applied mRNA sequencing (mRNA-seq) to further obtain the gene expression profile of the *Mll-Af9* pre-leukemic cells from the first plating after *Setd2* knockdown. Functional category enrichment analyses indicated that Setd2 deficiency activates gene expression in mTOR and Jak-Stat signaling pathways (Supplementary Fig. 15), which are known to contribute directly to leukemogenesis. Treatment of the *Setd2* knockdown pre-leukemic cells with the mTOR small-molecule inhibitor Torin1 or with rapamycin resulted in a marked decrease in cell growth (Fig. 4d and Supplementary Fig. 16). These data suggest that Setd2 downregulation enhances the leukemogenic potential of pre-leukemic cells by activation of multiple pathways, as exemplified by the mTOR signaling pathway.

To further determine the role of *Setd2* during the maintenance or progression of established leukemia, we obtained primary *Mll-Af9* or *MLL-NRIP3* leukemia cells from the leukemic mice (Figs. 1c and 5). *Setd2* knockdown significantly accelerated the development of both *Mll-Af9* and *MLL-NRIP3* leukemia in the serial transfer recipients, as evidenced by shortened latency and a more severe phenotype of the leukemia (Fig. 5a–c and Supplementary Fig. 13). The limiting dilution analysis of the transplanted mice showed a significantly higher frequency of leukemia-initiating cells or leukemia stem cells (LSCs) after *Setd2* knockdown (1/142 as compared to 1/2,765, $P = 0.001$, Fig. 5d), thereby providing direct evidence for increased self-renewal of LSCs through loss of function of *Setd2*. Consistently, when we examined the effect of *Setd2* knockdown on *MLL*-rearranged leukemia cells by mRNA-seq, gene set enrichment analysis (GSEA)[27] further indicated significantly higher expression of the human LSC signature[28], the human cancer-related embryonic stem cell signature[29,30] and the Wnt signaling pathway[31,32] (Fig. 5e and Supplementary Table 8) in the *Setd2* knockdown leukemia cells. These results provide strong evidence for the role of Setd2 downregulation in enhancing the stemness of LSCs, thereby contributing to the maintenance and progression of established leukemia.

In summary, given the recent flurry of reported mutations in chromatin regulatory genes in human tumors[33–39], a functional role of deregulated histone modification in cancer biology has not yet been established[40]. Our mutational analysis, together with *in vivo* and *in vitro* functional assays, demonstrates that loss of function of *SETD2* is a critical event in facilitating both disease initiation and progression through decreased H3K36me3 in leukemias characterized by *MLL* fusion, *MLL*-PTD or *AML1-ETO*. Thus, a *SETD2* mutation–mediated decrease of H3K36me3 may be an independent and distinct epigenetic mechanism to potentiate leukemic transformation and progression in cooperation with another genetic or epigenetic abnormality. How disruption of SETD2 cooperates with other pathogenic mechanisms, especially in promoting the stemness of LSCs, certainly warrants further investigations. Nonetheless, the existence of *SETD2* mutations in a range of hematopoietic malignancies as well as non-hematopoietic malignancies suggests that the SETD2-H3K36me3 pathway may be a common tumor-suppressive mechanism for cancer,

thereby offering a new opportunity for the development of cancer diagnostics and therapeutics.

Online Methods

Sample description and preparation of the monozygotic twin pair

A detailed case report is included in the Supplementary Note. In brief, a 3-year-old case was diagnosed as having AML FAB-M5 with *MLL* translocation on the basis of her clinical presentation, blood counts, morphology, FISH and cytometry analysis (Supplementary Fig. 1). The twin with *MLL*-rearranged leukemia (PT) and her healthy twin sibling (HT) were monozygotic twins, which was confirmed by a birth record from the hospital, genotyping of short tandem repeat (STR) loci and Amelogenin loci and STR-PCR analysis (Supplementary Fig. 2). FISH analysis did not detect *MLL* translocation in HT. According to the regulations of the institutional ethics review boards from the Institute of Hematology and Blood Diseases Hospital, Chinese Academy of Medical Sciences and Peking Union Medical College, informed consent was signed by the parents of the twins.

CD56$^+$CD64$^+$ leukemia cells (PT_Leukemia), CD56$^-$CD64$^-$ normal cells (PT_Normal) and normal PBMCs from HT were used for WGS and mRNA-seq. Sequencing was performed at the Core Genomic Facility of Beijing Institute of Genomics, Chinese Academy of Sciences. Genomic DNA libraries with a 1.5-kb insert size were prepared using genomic DNA extracted from PT_Leukemia and HT, followed by SOLiD mate-pair sequencing (50×2 bp). Three mRNA libraries with a 400-bp insert size were prepared using RNA harvested from PT_Leukemia, PT_Normal and HT, followed by paired-end sequencing (81×2 bp). All data were aligned to hg19 with Bioscope 1.3 (https://products.appliedbiosystems.com/ab/en/US/adirect/ab?cmd=catNavigate2&catID=606802&tab=Overview) and BWA[44], as summarized in Supplementary Table 1.

Detection of somatic mutations

We applied a series of in-house softwares to detect point mutations and structural variations on a whole-genome scale combining WGS and mRNA-seq data. In total, 623 SNVs (including 9 nonsynonymous SNVs and 1 splice-site SNV), 41 small indels, 3 large heterozygous deletions and 2 fusion genes were identified (a global view of all the genomic variations detected is shown in Fig. 1a and Supplementary Fig. 3, the 10 validated SNVs are presented in Supplementary Table 2 and Supplementary Fig. 8, all 623 SNVs and 41 small indels are shown in Supplementary Table 10, 3 large deletions are shown in Supplementary Fig. 6 and 2 validated fusion genes are shown in Supplementary Figs. 4 and 7).

Point variation (SNV and small indel) detection

Candidate SNVs were identified by CASpoint (an in-house software), which calculated the somatic score and two significance levels: one is calculated by one-side Fisher testing, which calculated the statistical significance in which the tumor mutant allele frequency (MAF) is higher than the MAF in the normal cell population; and the second uses binomial testing, which calculated the significance of the tumor mutant allele number observed from

the aligned tumor sequencing data, where the data meet a binomial distribution. Putative SNVs were identified using the following filtering criteria: (i) somatic score greater than 35; (ii) Fisher exact test (one tailed) P value for the mutant frequency between the tumor and normal tissue of less than 0.05; (iii) binomial test P value for the tumor alleles of less than 1×10^{-15}; (iv) tumor mutant allele number of at least 5; (v) Phred quality of the start point of the tumor covering the locus point larger than 1; (vi) tumor MAF greater than 0.2; and (vii) for a normal sample, a base quality of the reference allele larger than 30 and mapping quality of the reference allele larger than 35, and for a tumor sample, a base quality of the non-reference allele larger than 30 and mapping quality of the non-reference allele larger than 35. All filtering parameters were obtained from other in-house cancer projects.

We used SaMtools[45] to identify cancer-specific small indels. We set the total depth of one indel breakpoint to be at least 20 and the supporting reads rate to greater than 0.3 for the tumor sample and equal to 0 for the normal sample. After annotation, we found 41 leukemia-specific small indels, including 38 in intron and intergenic regions and 3 in UTRs.

Structural variation (CNV and fusion gene) detection

CAScnv (an in-house software) was used for detecting the somatic DNA CNV. We computed the number of reads aligned by Bioscope in the non-overlapping minimum sliding window (MSW), whose size is derived from CNV-seq[46]. We used the circular binary segmentation algorithm (CBS[47]) to segment CNV regions according to logarithm reads ratio (LRR)

$$\mathrm{LRR}=\log_2(R_\mathrm{C}/R_\mathrm{N} \times \gamma)$$

where R_C and R_N are read counts of cancer and normal DNA in each non-overlapping sliding window (1,500 MSWs as a sliding window) separately, and γ is the correction coefficient, which is the ratio of the read counts of normal and cancer DNA in a chromosome. From the above method, we divided the genome into contiguous regions according to the segmentation significance level ($P < 1 \times 10^{-5}$). We detected three large heterozygous deletions, one in chromosome 6 and two in chromosome 7, and validated them by genotyping loss of heterozygosity (LOH) sites predicted from the WGS data (Supplementary Fig. 6).

Candidate leukemia-specific gene fusion events were identified by CASfus (an in-house software), which is used for detecting interchromosomal or intra-chromosomal gene fusions from genome sequencing data. CASfus locates fusion candidate regions from inappropriate read pairs aligned in different gene loci according to annotation, assembles all the reads around these regions into contigs and then realigns them to detect potential fusion events. CASbreak (an in-house software) was used to detect cancer-specific breakpoints. We detected two leukemia-specific fusion events, *MLL-NRIP3* and *NF1-AARSD1*, from WGS data by crossvalidation with CASfus and CASbreak and verified them with mRNA-seq and PCR sequencing (Fig. 1b, Supplementary Note, Supplementary Table 11 and Supplementary Figs. 4 and 7).

SETD2 mutation screening in patients with acute leukemia using targeted sequencing

To determine the recurrence of *SETD2* mutations, we collected 134 patients with AML and 107 patients with ALL (Supplementary Note). According to the regulations of the institutional ethics review boards from the Institute of Hematology and Blood Diseases Hospital, Chinese Academy of Medical Sciences and Peking Union Medical College, TongJi Hospital, TongJi Medical College, HuaZhong University of Science and Technology and Changhai Hospital, Second Military Medical University, informed consent was signed by the parents or guardians of the patients. We amplified all 21 exons of *SETD2* with a set of PCR primers designed by Primer 5.0 with the default parameters (Supplementary Table 12) and performed Sanger sequencing on PCR amplicons from the 241 leukemia samples. After eliminating known polymorphisms reported in the dbSNP database (build 131)[48], the Korean genome[49], the YanHuang database[50], the 1000 human genome polymorphism data set[51] (1000 Genomes) and the Exome Variant Server (http://evs.gs.washington.edu/EVS/), we obtained candidate somatic mutations. We further confirmed somatic mutations if they were present in tumor cells but were undetectable in any available matched normal control cells (skin, saliva, mesenchymal stem cells or remission PBMCs) by PCR sequencing. When matched normal control tissues were not available, the candidate variants were classified as very probable somatic mutations if they were not among the 146 *SETD2* polymorphisms found in 950 normal individuals (257 Asian and 693 non-Asian) in the collected data sets. Clinical and mutational information for the patients with leukemia is summarized in Supplementary Tables 3–6.

SETD2 deletion detection based on gene expression array data

To determine the deletion pattern across *SETD2*, we used an established genomic method[13,14] to analyze large deletions in seven gene expression data sets consisting of individuals with AML or ALL and normal individuals by global gene expression meta-analysis. In brief, we compared the gene expression profile of each individual to a reference baseline made up of a large number of highly similar samples. For each sample, the expression value of each gene was divided by the median expression value of the same gene across the entire data set. A detailed description of the method can be found in the studies of Mayshar *et al.*[13,14]. First, we validated the methodology for inferring large deletions based on transcriptional profiling using deletions detected by SNP array in a cohort of patients with chronic lymphocytic leukemia, in which both SNP and gene expression analyses had been conducted[52] (Supplementary Fig. 17). Second, we used a cohort of patients with ccRCC[15] with SNP array and expression array data to test the power of detecting large deletions across the *SETD2* genomic region (chromosome 3p) with the expression array. The results demonstrated that the expression analysis detected chromosome 3p deletion at a similar frequency as that identified by the SNP array data (Supplementary Fig. 12). Third, using the same genomic analysis method, large genomic deletions encompassing *SETD2* were detected in patients with *MLL* fusion, as well as patients with either *TEL-AML1* or *BCR-ABL*, but at a very low frequency (0.6%) (Supplementary Fig. 11 and Supplementary Table 7).

Confirming rare deletion across *SETD2* using LOH detection in chromosome 3p

To further confirm the rare *SETD2* deletion pattern obtained from the expression-based genomic analysis described above, we used the MassARRAY system (Sequenom) to detect LOH of chromosome 3p in our cohort of patients with acute leukemia. Sequenom genotyping has been used to detect LOH across known tumor-suppressor genes, especially for chromosome 3p[53–55], as a locus is very likely to have LOH if it contains continuous homozygous SNPs. Each SNP is defined as homozygous or heterozygous on the basis of Sequenom genotyping. In total, we selected 69 SNPs (63 on chromosome 3 and 6 on other chromosomes) with MAFs ranging from 0.3 to 0.7 in the 1000 Genomes data. Thirty-five out of 47 SNPs located on chromosome 3p are within the *SETD2* locus. On average, these 63 sites on chromosome 3 space about 1 kb and 4 Mb within and outside the *SETD2* locus, respectively. Amplification and extension primers for Sequenom genotyping were designed using Human GenoTyping Tools on the MySequenom website (https:// www.mysequenom.com/) and MassARRAY Assay Design v3.1 software.

On the basis of targeted sequencing of *SETD2* in the 241 patients with leukemia, 69 patients without any heterozygous SNPs in exonic regions of *SETD2* were selected as candidates for LOH screening. We also selected 19 negative controls with multiple (5) heterozygous SNPs in exonic regions of *SETD2*. We genotyped all 69 selected SNPs for 30 out of 69 *SETD2* LOH candidates and 10 out of 19 negative controls according to the Sequenom standard protocol. Genotype calls were automatically generated according to signal characteristics[56]. Results were then linked to plate information created by MassARRAY Typer 4.0 software. Individual calls and their MAFs were manually reviewed and finalized.

We further selected all 254 Asians from the 1000 Genomes data as a control set to test whether the amount of *SETD2* LOH in the leukemia cohort is significantly different from that of the healthy population. We extracted MAFs from the 1000 Genomes data for 18 SNPs identified by targeted sequencing of *SETD2* and 69 SNPs used in the genotyping for detecting chromosome 3 LOH. A similar pattern of LOH in *SETD2* was observed between the leukemia cohort and the healthy Asian population. Then, using neutral LOH testing, we concluded that the same frequency (26-29%) of LOH across *SETD2* is due to linkage disequilibrium (http://hapmap.ncbi.nlm.nih.gov/cgi-perl/gbrowse/hapmap24_B36/#search) rather than deletion in the *SETD2* locus (Supplementary Fig. 10a). This finding is consistent with the rare *SETD2* deletion detected by large-scale expression genomic analysis (Supplementary Fig. 11 and Supplementary Table 7).

DNA methylation analysis of the *SETD2* promoter

To examine whether the *SETD2* promoter is hypermethylated in patients with acute leukemia, we obtained available Human DNA Methylation450 array data of 194 AML and 301 ccRCC samples from TCGA (https://tcga-data.nci.nih.gov/tcga/tcgaHome2.jsp). We used the level 3 methylation data defined by TCGA, which is the ratio of the intensity of the methylated probe to the total intensity of the methylated and unmethylated probes for each CpG site. Therefore, a β value ranges between 0 (least methylated) and 1 (most methylated), which represents the degree of methylated state of any particular locus. The data contain null entries, which correspond to probes that overlap with known SNPs or other genomic

variations and probes whose signal intensities are lower than the background. For each gene, we defined its promoter as the region starting 5 kb upstream and ending 1 kb downstream of the annotated transcription start site based on UCSC gene annotations (release on April 8, 2013). We filtered out probes with many null entries (i.e., number of null entries over 1% of the sample size) and those located outside of gene promoters. 196,896 CpG probes remained for further analysis. The β values of all CpG sites located in each promoter were averaged as the DNA methylation level of this promoter. Promoter DNA methylation of all genes in 194 patients with AML were examined (Supplementary Fig. 10d). We also visualized the DNA methylation levels of *SETD2*, *BAP1*, *KDM6A*, *PBRM1*, *PDZD2* and *TP73* in patients with AML or ccRCC (Supplementary Fig. 10e). Among these genes, *SETD2*, *BAP1*, *KDM6A* and *PBRM1* are known to be unmethylated in patients with ccRCC[57], and *FDZD2* and *TP73* have been shown to be hypermethylated in patients with hematopoietic malignancies[58,59].

Mutational pattern analysis of cancer-causative genes and *SETD2*

The gene-truncating mutation rate (F_T) is the ratio of the number of patients with truncating mutations in a certain gene to the number of patients with non-synonymous or frameshift small indel (coding) mutations in that gene. The gene multi-hit rate (F_{MH}) is the ratio of the number of patients with at least one truncating mutation and one other coding mutation of a certain gene to the number of patients with coding mutations in that gene. We calculated the F_T and F_{MH} of cancer-causative genes using mutations in the COSMIC database (release 65). For *SETD2*, we calculated F_T and F_{MH} using mutations in the COSMIC data set combined with data sets provided by Zhang *et al.*[39] and data sets from this study. The results for all genes analyzed are shown in Supplementary Table 13.

Plasmid, cell transfection and lentivirus transduction

The SF-LV-shRNA-GFP and SF-LV-shRNA-BFP plasmids were obtained from K.L. Rudolph's lab[60], scrambled shRNA was cloned from TRIPZ non-silencing shRNA (Open Biosystems, RHS4743) and *Setd2* shRNAs were cloned from GIPZ mouse *Setd2* shRNA (Open Biosystems, RMM4532). Lentiviruses (SF-LV-scramble-GFP and SF-LV-shSetd2-GFP) were generated by co-transfecting the packaging plasmids sPAX2 and MD2.G into 293T cells by Fugene 6 (Promega, E2691). The *MLL-NRIP3* fusion gene was subcloned into the pMIG-IRES-GFP vector. For viral production, the pMIG-*MLL-NRIP3* or empty control vector was co-transfected into the 293T packaging cell line with pCMV-VSVG and pKat. The lentivirus supernatants were collected 42 h after transfection, filtered through a 0.45-μm filter and used immediately to infect overnight-cultured bone marrow (BM) cells.

Colony-forming assay

One milliliter of colony assay medium (MethoCult GF M3434, Stem Cell Technologies) contained 1×10^4 GFP$^+$ cells, which were sorted from mouse BM cells infected with lentiviruses. The cells were plated in 35-mm dishes (Nunc). Each sample was plated in triplicate. Colony counts were scored, and re-platings occurred every 7 d.

In vitro long-term liquid culture

Knock-in mouse BM cells were harvested and infected with lentiviruses. 1×10^4 or 2×10^4 GFP+ cells were sorted and cultured in Iscove's modified Dulbecco's medium (IMDM) with 10% FBS and cytokines (SCF, GM-CSF, IL-3 and IL-6), and each sample was plated in duplicate wells. Cell counts and passages were repeated every 7 d.

Inhibitor treatment experiment

Knock-in mouse BM cells were harvested and infected with lentiviruses. 1×10^4 GFP+ cells were sorted and cultured in IMDM with 10% FBS and cytokines (SCF, GM-CSF, IL-3 and IL-6) and various concentrations of inhibitors in a 24-well plate, and each sample was plated in duplicate. Cumulative cells were counted 48 h after drug treatment.

Mouse and BMT assay

Animals were housed in the animal barrier facility at Cincinnati Children's Hospital Medical Center or the Institute of Hematology, Chinese Academy of Medical Sciences. All animal studies were conducted according to an approved Institutional Animal Care and Use Committee protocol at both institutions. Randomized C57BL/6J mice with aged 2–4 months were used, and experimenters that harvested mice for BMT were double blinded. Mycoplasma contamination was always negative using regular examination.

Mll-Af9 (ref. 22), *Mll*-PTD[23] or *Aml1-Eto*[24] knock-in mice were injected with 5-fluorouracil (5-FU) (150 mg per kg body weight), and BM cells were harvested 4 d after injection. Mononuclear cells were isolated by density gradient centrifugation. BMTs were performed as described[61]. Briefly, lethally or sublethally irradiated recipients were reconstituted with *Setd2* shRNA–infected BM cells or *Mll-Af9* leukemic cells. Secondary or tertiary transplantations were performed with GFP+ BM cells sorted from the first or secondary transplantation recipients when they became morbid. Female and male mice were used for recipients and donors, respectively.

MLL-NRIP3 AML was generated by injection of *MLL-NRIP3*–transduced BM cells into lethally irradiated syngeneic recipient mice. Primary *MLL-NRIP3* leukemia cells were transduced with SF-LV-shSetd2-BFP lentiviruses or SF-LV-scramble-BFP lentiviruses. GFP and BFP double-positive cells were sorted and injected into sublethally irradiated recipients. Serial transplantation was performed to determine the self-renewal potential of the established leukemia cells. Almost all of the mice used for serial BMT were female.

Limited dilution assay

GFP+ *Mll-Af9* knock-in BM cells were sorted from the primary transplantation recipients when they became morbid. 250,000 CD45.1+ helper cells mixed with 100,000, 10,000, 1,000 or 100 GFP+ BM cells were injected to lethally irradiated CD45.1 congenic recipient mice (Supplementary Table 9).

Western blot (WB) analysis

PBMCs from the cohort of patients with leukemia and GFP+-sorted *Mll-Af9* knock-in BM cells were used for WB analysis. One million cells were lysed with 50 μl 2× SDS sample

buffer, sonicated for 20 s and then boiled at 95 °C for 5 min. These whole-cell extractions were resolved by SDS-PAGE and electrotransferred to polyvinylidene difluoride membranes (Millipore). The following primary antibodies were used in this study: anti-SETD2 (Aviva, ARP47617_T100, 1:500), anti-H3 (Abcam, ab1791, 1:30,000), anti-H3K36me3 (Abcam, ab9050, 1:4,000), anti-H3K79me2 (Abcam, ab3594, 1:1,000) and anti-H3K27me3 (Abcam, ab6002, 1:1,000). Horseradish peroxidase–conjugated antibodies to rabbit (GE, NA934V, 1:6,000) were used as the secondary antibody, and SuperSignal West Dura Chemiluminescent Substrate (Pierce) was used for detection.

mRNA expression analysis

mRNA-seq was performed to profile mRNA expression levels in *Setd2* knockdown HSPCs and scrambled control HSPCs from the first plating in the *Mll-Af9* knock-in mouse model and from the serial BMT *MLL-NRIP3* mouse model. *Setd2* knockdown with two different shRNAs was performed for each HSPC from the *Mll-Af9* knock-in mouse model or *MLL-NRIP3* mouse model. mRNA-seq reads were aligned to the mm9 reference sequence using BWA[44] or TopHat[62] algorithms with a tolerance of three mismatches. Then we used Cuffdiff[62] to perform differential expression testing to detect the differentially expressed genes. Genes with $q < 0.05$ were defined to be statistically differentially expressed. Then the differentially expressed genes identified were used for pathway enrichment analysis with DAVID Bioinformatics resources[63]. Gene lists, including KEGG pathway signatures and stem cell signatures, were obtained from the GSEA[27] MSigDB website (http://www.broadinstitute.org/gsea/msigdb/index.jsp) for GSEA analysis in our mRNA expression data.

Statistical analyses and data visualization

All statistical tests were performed using GraphPad Prism 5 and the R statistical software package. Survival curves were compared using GraphPad Prism 5 by Kaplan-Meier analysis followed by log-rank (Mantel-Cox) test comparison. Statistical comparisons between two groups (*Setd2* knockdown compared to scrambled control) were performed in GraphPad Prism 5 using an unpaired, two-tailed Student's *t* test; equal variances were not assumed. Data were visualized by using GraphPad Prism 5, Microsoft Visio 2007, Microsoft Excel, Microsoft PowerPoint and the R statistical software package.

Supplementary Material

Refer to Web version on PubMed Central for supplementary material.

Acknowledgments

References

1. Krivtsov AV, Armstrong SA. *MLL* translocations, histone modifications and leukaemia stem-cell development. Nat Rev Cancer. 2007; 7:823–833. [PubMed: 17957188]

2. Cancer Genome Atlas Research Network. Genomic and epigenomic landscapes of adult de novo acute myeloid leukemia. N Engl J Med. 2013; 368:2059–2074. [PubMed: 23634996]

3. Balgobind BV, et al. *NRIP3*: a novel translocation partner of *MLL* detected in a pediatric acute myeloid leukemia with complex chromosome 11 rearrangements. Haematologica. 2009; 94:1033. [PubMed: 19454493]

4. Sun XJ, et al. Identification and characterization of a novel human histone H3 lysine 36–specific methyltransferase. J Biol Chem. 2005; 280:35261–35271. [PubMed: 16118227]

5. Zhang Y, Rowley JD. Chromatin structural elements and chromosomal translocations in leukemia. DNA Repair (Amst). 2006; 5:1282–1297. [PubMed: 16893685]

6. Zhang Y, et al. The role of mechanistic factors in promoting chromosomal translocations found in lymphoid and other cancers. Adv Immunol. 2010; 106:93–133. [PubMed: 20728025]

7. Mitelman F, Johansson B, Mertens F. The impact of translocations and gene fusions on cancer causation. Nat Rev Cancer. 2007; 7:233–245. [PubMed: 17361217]

8. Balgobind BV, Zwaan CM, Pieters R, Van den Heuvel-Eibrink MM. The heterogeneity of pediatric *MLL*-rearranged acute myeloid leukemia. Leukemia. 2011; 25:1239–1248. [PubMed: 21566656]

9. Greaves MF, Wiemels J. Origins of chromosome translocations in childhood leukaemia. Nat Rev Cancer. 2003; 3:639–649. [PubMed: 12951583]

10. Edmunds JW, Mahadevan LC, Clayton AL. Dynamic histone H3 methylation during gene induction: HYPB/Setd2 mediates all H3K36 trimethylation. EMBO J. 2008; 27:406–420. [PubMed: 18157086]

11. Berger SL. The complex language of chromatin regulation during transcription. Nature. 2007; 447:407–412. [PubMed: 17522673]

12. Liu H, Xing Y, Yang S, Tian D. Remarkable difference of somatic mutation patterns between oncogenes and tumor suppressor genes. Oncol Rep. 2011; 26:1539–1546. [PubMed: 21887471]

13. Mayshar Y, et al. Identification and classification of chromosomal aberrations in human induced pluripotent stem cells. Cell Stem Cell. 2010; 7:521–531. [PubMed: 20887957]

14. Ben-David U, Mayshar Y, Benvenisty N. Large-scale analysis reveals acquisition of lineage-specific chromosomal aberrations in human adult stem cells. Cell Stem Cell. 2011; 9:97–102. [PubMed: 21816361]

15. Dondeti VR, et al. Integrative genomic analyses of sporadic clear cell renal cell carcinoma define disease subtypes and potential new therapeutic targets. Cancer Res. 2012; 72:112–121. [PubMed: 22094876]

16. Cancer Genome Atlas Research Network. Comprehensive molecular characterization of clear cell renal cell carcinoma. Nature. 2013; 499:43–49. [PubMed: 23792563]

17. Rhodes DR, et al. Oncomine 3.0: genes, pathways, and networks in a collection of 18,000 cancer gene expression profiles. Neoplasia. 2007; 9:166–180. [PubMed: 17356713]

18. Li M, et al. Solution structure of the Set2-Rpb1 interacting domain of human Set2 and its interaction with the hyperphosphorylated C-terminal domain of Rpb1. Proc Natl Acad Sci USA. 2005; 102:17636–17641. [PubMed: 16314571]

19. Duns G, et al. Histone methyltransferase gene *SETD2* is a novel tumor suppressor gene in clear cell renal cell carcinoma. Cancer Res. 2010; 70:4287–4291. [PubMed: 20501857]

20. Fontebasso AM, et al. Mutations in *SETD2* and genes affecting histone H3K36 methylation target hemispheric high-grade gliomas. Acta Neuropathol. 2013; 125:659–669. [PubMed: 23417712]

21. Fontebasso AM, et al. Mutations in *SETD2* and genes affecting histone H3K36 methylation target hemispheric high-grade gliomas. Acta Neuropathol. 2009; 125:659–487. [PubMed: 23417712]

22. Corral J, et al. An *Mll-AF9* fusion gene made by homologous recombination causes acute leukemia in chimeric mice: a method to create fusion oncogenes. Cell. 1996; 85:853–861. [PubMed: 8681380]

23. Dorrance AM, et al. *Mll* partial tandem duplication induces aberrant *Hox* expression *in vivo* via specific epigenetic alterations. J Clin Invest. 2006; 116:2707–2716. [PubMed: 16981007]

24. Higuchi M, et al. Expression of a conditional *AML1-ETO* oncogene bypasses embryonic lethality and establishes a murine model of human t(8;21) acute myeloid leukemia. Cancer Cell. 2002; 1:63–74. [PubMed: 12086889]

25. Zorko NA, et al. *Mll* partial tandem duplication and *Flt3* internal tandem duplication in a double knock-in mouse recapitulates features of counterpart human acute myeloid leukemias. Blood. 2012; 120:1130–1136. [PubMed: 22674806]

26. Grisolano JL, O'Neal J, Cain J, Tomasson MH. An activated receptor tyrosine kinase, TEL/PDGFβR, cooperates with AML1/ETO to induce acute myeloid leukemia in mice. Proc Natl Acad Sci USA. 2003; 100:9506–9511. [PubMed: 12881486]

27. Subramanian A, et al. Gene set enrichment analysis: a knowledge-based approach for interpreting genome-wide expression profiles. Proc Natl Acad Sci USA. 2005; 102:15545–15550. [PubMed: 16199517]

28. Gal H, et al. Gene expression profiles of AML derived stem cells; similarity to hematopoietic stem cells. Leukemia. 2006; 20:2147–2154. [PubMed: 17039238]

29. Wong DJ, et al. Module map of stem cell genes guides creation of epithelial cancer stem cells. Cell Stem Cell. 2008; 2:333–344. [PubMed: 18397753]

30. Wang Y, Armstrong SA. Cancer: inappropriate expression of stem cell programs? Cell Stem Cell. 2008; 2:297–299. [PubMed: 18397746]

31. Wang Y, et al. The Wnt/β-catenin pathway is required for the development of leukemia stem cells in AML. Science. 2010; 327:1650–1653. [PubMed: 20339075]

32. Kanehisa M, Goto S, Sato Y, Furumichi M, Tanabe M. KEGG for integration and interpretation of large-scale molecular data sets. Nucleic Acids Res. 2012; 40:D109–D114. [PubMed: 22080510]

33. Gerlinger M, et al. Intratumor heterogeneity and branched evolution revealed by multiregion sequencing. N Engl J Med. 2012; 366:883–892. [PubMed: 22397650]

34. Gui Y, et al. Frequent mutations of chromatin remodeling genes in transitional cell carcinoma of the bladder. Nat Genet. 2011; 43:875–878. [PubMed: 21822268]

35. Varela I, et al. Exome sequencing identifies frequent mutation of the SWI/SNF complex gene *PBRM1* in renal carcinoma. Nature. 2011; 469:539–542. [PubMed: 21248752]

36. Dalgliesh GL, et al. Systematic sequencing of renal carcinoma reveals inactivation of histone modifying genes. Nature. 2010; 463:360–363. [PubMed: 20054297]

37. Zang ZJ, et al. Exome sequencing of gastric adenocarcinoma identifies recurrent somatic mutations in cell adhesion and chromatin remodeling genes. Nat Genet. 2012; 44:570–574. [PubMed: 22484628]

38. Fujimoto A, et al. Whole-genome sequencing of liver cancers identifies etiological influences on mutation patterns and recurrent mutations in chromatin regulators. Nat Genet. 2012; 44:760–764. [PubMed: 22634756]

39. Zhang J, et al. The genetic basis of early T-cell precursor acute lymphoblastic leukaemia. Nature. 2012; 481:157–163. [PubMed: 22237106]

40. Ryan RJ, Bernstein BE. Molecular biology. Genetic events that shape the cancer epigenome. Science. 2012; 336:1513–1514. [PubMed: 22723401]

41. Krzywinski M, et al. Circos: an information aesthetic for comparative genomics. Genome Res. 2009; 19:1639–1645. [PubMed: 19541911]

42. Humphrey W, Dalke A, Schulten K. VMD: visual molecular dynamics. J Mol Graph. 1996; 14:33–38. [PubMed: 8744570]

43. Schneider CA, Rasband WS, Eliceiri KW. NIH Image to ImageJ: 25 years of image analysis. Nat Methods. 2012; 9:671–675. [PubMed: 22930834]

44. Li H, Durbin R. Fast and accurate short read alignment with Burrows-Wheeler transform. Bioinformatics. 2009; 25:1754–1760. [PubMed: 19451168]

45. Li H, et al. The Sequence Alignment/Map format and SAMtools. Bioinformatics. 2009; 25:2078–2079. [PubMed: 19505943]

46. Xie C, Tammi MT. CNV-seq, a new method to detect copy number variation using high-throughput sequencing. BMC Bioinformatics. 2009; 10:80. [PubMed: 19267900]

47. Olshen AB, Venkatraman ES, Lucito R, Wigler M. Circular binary segmentation for the analysis of array-based DNA copy number data. Biostatistics. 2004; 5:557–572. [PubMed: 15475419]

48. Sherry ST, et al. dbSNP: the NCBI database of genetic variation. Nucleic Acids Res. 2001; 29:308–311. [PubMed: 11125122]

49. Ahn SM, et al. The first Korean genome sequence and analysis: full genome sequencing for a socio-ethnic group. Genome Res. 2009; 19:1622–1629. [PubMed: 19470904]

50. Li G, et al. The YH database: the first Asian diploid genome database. Nucleic Acids Res. 2009; 37:D1025–D1028. [PubMed: 19073702]

51. Abecasis GR, et al. A map of human genome variation from population-scale sequencing. Nature. 2010; 467:1061–1073. [PubMed: 20981092]

52. Mosca L, et al. Integrative genomics analyses reveal molecularly distinct subgroups of B-cell chronic lymphocytic leukemia patients with 13q14 deletion. Clin Cancer Res. 2010; 16:5641–5653. [PubMed: 20947517]

53. Tai AL, et al. High-throughput loss-of-heterozygosity study of chromosome 3p in lung cancer using single-nucleotide polymorphism markers. Cancer Res. 2006; 66:4133–4138. [PubMed: 16618734]

54. Onken MD, et al. Loss of heterozygosity of chromosome 3 detected with single nucleotide polymorphisms is superior to monosomy 3 for predicting metastasis in uveal melanoma. Clin Cancer Res. 2007; 13:2923–2927. [PubMed: 17504992]

55. Angeloni D. Molecular analysis of deletions in human chromosome 3p21 and the role of resident cancer genes in disease. Brief Funct Genomic Proteomic. 2007; 6:19–39. [PubMed: 17525073]

56. Arcila M, Lau C, Nafa K, Ladanyi M. Detection of *KRAS* and *BRAF* mutations in colorectal carcinoma roles for high-sensitivity locked nucleic acid–PCR sequencing and broad-spectrum mass spectrometry genotyping. J Mol Diagn. 2011; 13:64–73. [PubMed: 21227396]

57. Ibragimova I, Maradeo ME, Dulaimi E, Cairns P. Aberrant promoter hypermethylation of *PBRM1*, *BAP1*, *SETD2*, *KDM6A* and other chromatin-modifying genes is absent or rare in clear cell RCC. Epigenetics. 2013; 8:486–493. [PubMed: 23644518]

58. Figueroa ME, et al. DNA methylation signatures identify biologically distinct subtypes in acute myeloid leukemia. Cancer Cell. 2010; 17:13–27. [PubMed: 20060365]

59. Zhao Y, et al. Aberration of p73 promoter methylation in *de novo* myelodysplastic syndrome. Hematology. 2012; 17:275–282. [PubMed: 22971533]

60. Wang J, et al. A differentiation checkpoint limits hematopoietic stem cell self-renewal in response to DNA damage. Cell. 2012; 148:1001–1014. [PubMed: 22385964]

61. Zhang Y, et al. Stress hematopoiesis reveals abnormal control of self-renewal, lineage bias, and myeloid differentiation in Mll partial tandem duplication (Mll-PTD) hematopoietic stem/progenitor cells. Blood. 2012; 120:1118–1129. [PubMed: 22740449]

62. Trapnell C, et al. Differential gene and transcript expression analysis of RNA-seq experiments with TopHat and Cufflinks. Nat Protoc. 2012; 7:562–578. [PubMed: 22383036]

63. Huang W, Sherman BT, Lempicki RA. Systematic and integrative analysis of large gene lists using DAVID bioinformatics resources. Nat Protoc. 2009; 4:44–57. [PubMed: 19131956]
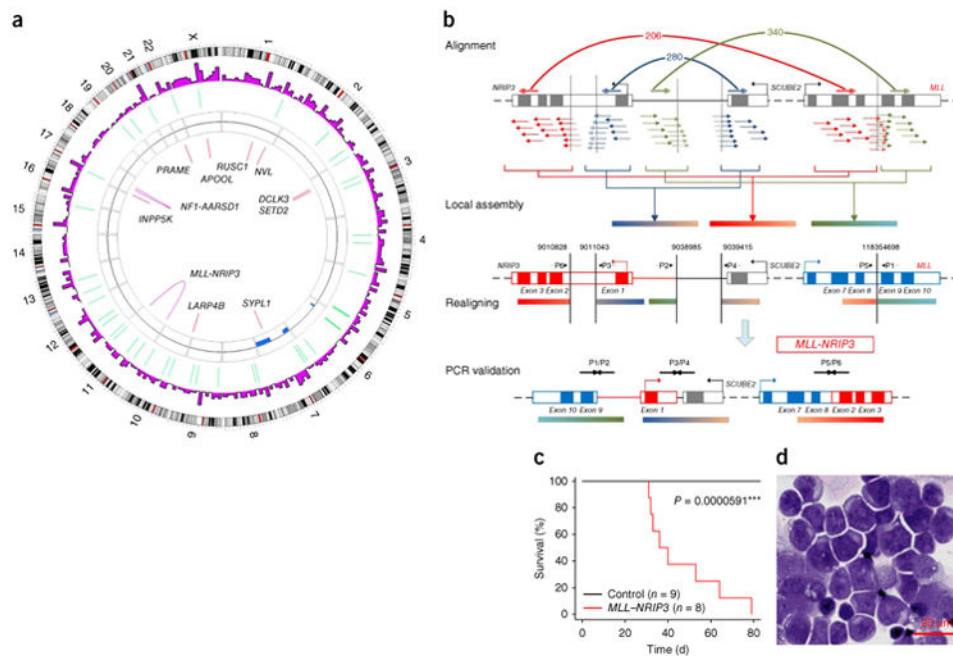
Figure 1.
Mutational and functional analysis of the *MLL-NRIP3* fusion gene identified a monozygotic twin pair discordant for *MLL*-rearranged leukemia. (**a**) Circos[41] plot showing the genetic alterations identified in the twin with leukemia, using the healthy twin as a normal control. Genes with validated coding single-nucleotide variants (SNVs) and fusion genes are indicated. CNV, copy-number variation. (**b**) Genetic events in the formation of the *MLL-NRIP3* fusion gene. Sequencing reads, shown as groups of short arrows, were aligned onto the non-rearranged *MLL-NRIP3* locus on chromosome 11 (top row, labeled alignment). Paired reads mapped onto six non-continued regions were identified and assembled into three contigs (second row, labeled local assembly). Non-continued regions connected by paired reads are joined by a bracket (below the *MLL-NRIP3* locus) and a curved line (above the *MLL-NRIP3* locus), with the numbers of supportive paired reads shown The three assembled contigs were realigned onto the non-rearranged loci to identify potential chromosomal break points, which are indicated by five vertical lines (third row, labeled realigning). The rearranged *MLL-NRIP3* locus was assembled. PCR primers (P1/P2, P3/P4 and P5/P6) were designed to confirm the fusion conjunctions resulting from the chromosomal rearrangements (fourth row, labeled PCR validation, and supplementary Fig. 4). (**c**) Survival curve for recipients of the bone marrow cells transduced with *MLL-NRIP3* or the empty vector control ($P = 5.91 \times 10^{-5}$, Mantel-Haenszel test). *MLL-NRIP3* induced myeloid leukemia with a median survival of 46.5 days. (**d**) Immature myeloblasts are shown by the morphology of the bone marrow biopsy specimen from a mouse with *MLL-NRIP3* leukemia. Throughout the figures, * indicates significance passing the threshold of $P < 0.05$ ** indicates passing the threshold of $P < 0.01$, and *** indicates passing the threshold of $P < 0.001$.
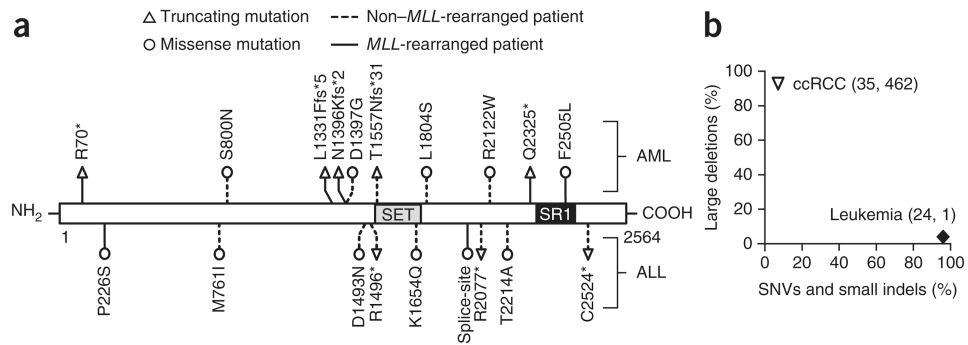
Figure 2.
Mutational analysis of *SETD2* in patients with acute leukemia. (**a**) *SETD2* mutations in patients with acute leukemia. The locations of the SET and SRI domains of *SETD2* are indicated. The type and position of each identified mutation is shown. HGVS notations corresponding to the abbreviations of the *SETD2* mutations used here are listed in Supplementary Table 3. (**b**) Distinct mutation spectrum of *SETD2* in patients with either acute leukemia or ccRCC. Mutational information of *SETD2* was obtained from the current study, a previous report by Zhang *et al.*[39] and the TCGA Research Network[16]. The percentages of SNVs, small insertions or deletions (indels) and large deletions in *SETD2* are shown, with the number of each of these variants in parentheses.
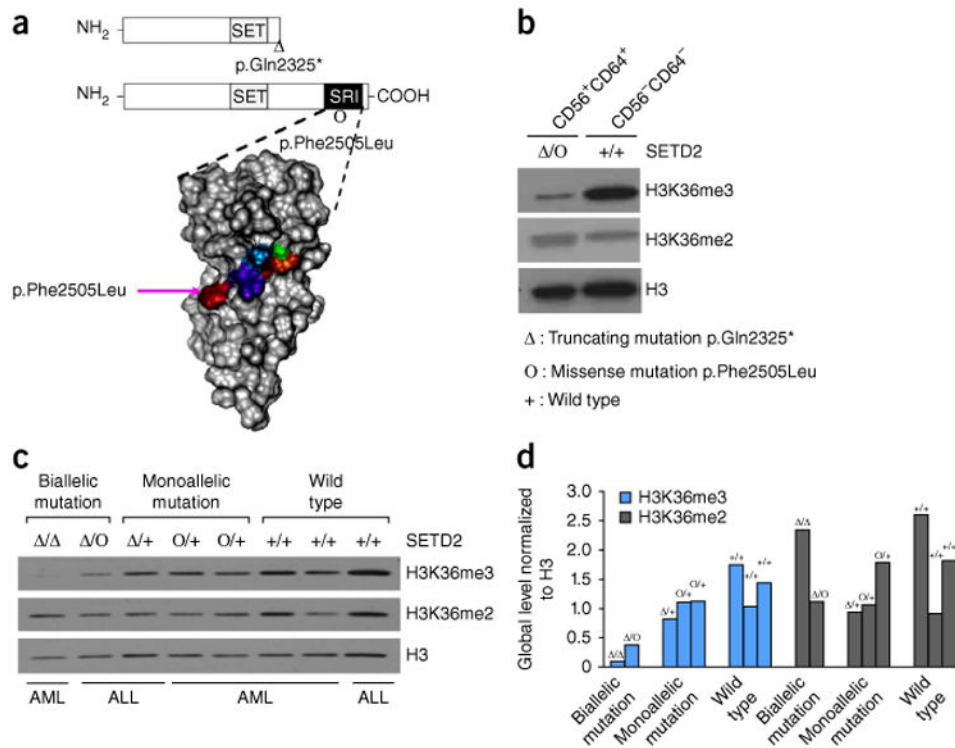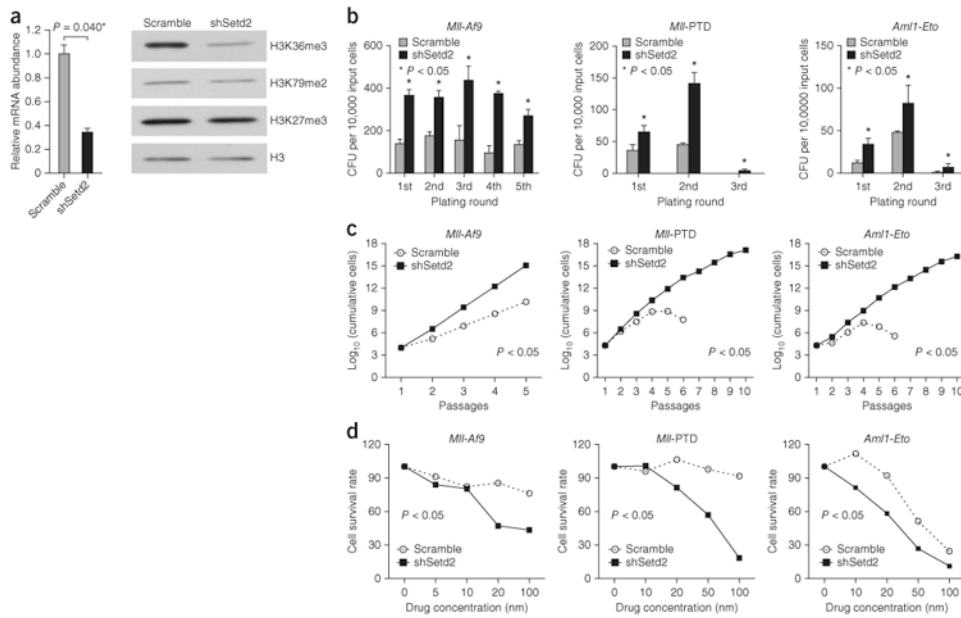
Figure 3.
H3K36me3 levels in patients with acute leukemia carrying *SETD2* mutations. (**a**) Two *SETD2* point mutations identified in the twin with leukemia. The nonsense mutation resulting in p.Gln2325* is expected to truncat the C terminus RNA Pol II–interacting SRI domain (top). The position of the missense mutation resulting in p.Phe2505Leu is also indicated. Below, surface mapping shows the five key residues (colored) located on the surface of the SRI domain that are critical for the interaction of the SRI domain with RNA Pol II[18]. The SRI domain of SETD2 was visualized by VMD[42], and p.Phe2505Leu is marked with a pink arrow. (**b**) Global H3K36me3 and H3K36me2 levels in leukemic cells isolated from the twin with leukemia. The leukemic (CD56$^+$CD64$^+$) and normal (CD56$^-$CD64$^-$) cell populations were isolated from the twin with leukemia, and the *SETD2* mutational status for each population is indicated. Global H3K36me3 and H3K36me2 levels were detected by western blot assays. Histone H3 was used as a loading control. (**c**) Global H3K36me3 and H3K36me2 levels in leukemic cells isolated from patients with either AML or ALL detected by western blot assays. The *SETD2* mutational status for each patient is indicated. H3 was used as a loading control. (**d**) The signal intensity of each band in c was quantified by ImageJ[43]. The intensities of H3K36me3 and H3K36me2 were normalized to that of H3 for each lane and are shown in a bar plot. The *SETD2* mutational status for each patient is indicated.

Figure 4.
Functional analysis of *Setd2* in pre-leukemic cells. (**a**) Knockdown of *Setd2* in HSPCs derived from *Mll-Af9* knock-in mice. The bar plot shows the relative *Setd2* expression (mean ± s.d.; $n = 2$ per group; Student's *t* test) in *Mll-Af9* HSPCs transduced with *Setd2* shRNA (shSetd2) or the scrambled control shRNA (scramble). The western blot shows the global levels of H3K36me3, H3K79me2 and H3K37me3 in these cells. (**b**) Serial colony-forming unit (CFU) re-plating assays for HSPCs derived from *Mll-Af9*, *Mll*-PTD and *Aml1-Eto* knock-in mice. Cells were treated with either *Setd2* shRNA or the control scrambled shRNA. The plating round and the number of CFUs per 10,000 input cells are shown (mean ± s.d.; $n = 3$ per group; Student's *t* test). (**c**) Serial liquid culture assays for HSPCs derived from *Mll-Af9*, *Mll*-PTD and *Aml1-Eto* knock-in mice. Cells were treated with either *Setd2* shRNA or control scrambled shRNA. The number of passages and the $\log_{10}$-transformed number of cumulative cells are shown ($n = 5$ or 10; Student's *t* test for comparison between two groups). (**d**) Increased sensitivity to mTOR inhibition by Torin1 in *Setd2* knockdown HSPCs isolated from *Mll-Af9*, *Mll*-PTD and *Aml1-Eto* knock-in mice. *Setd2* knockdown or scrambled shRNA–transduced cells were plated ($n = 5$; Student's *t* test for comparison between two groups). The mTOR inhibitor Torin1 was added at the indicated concentrations.
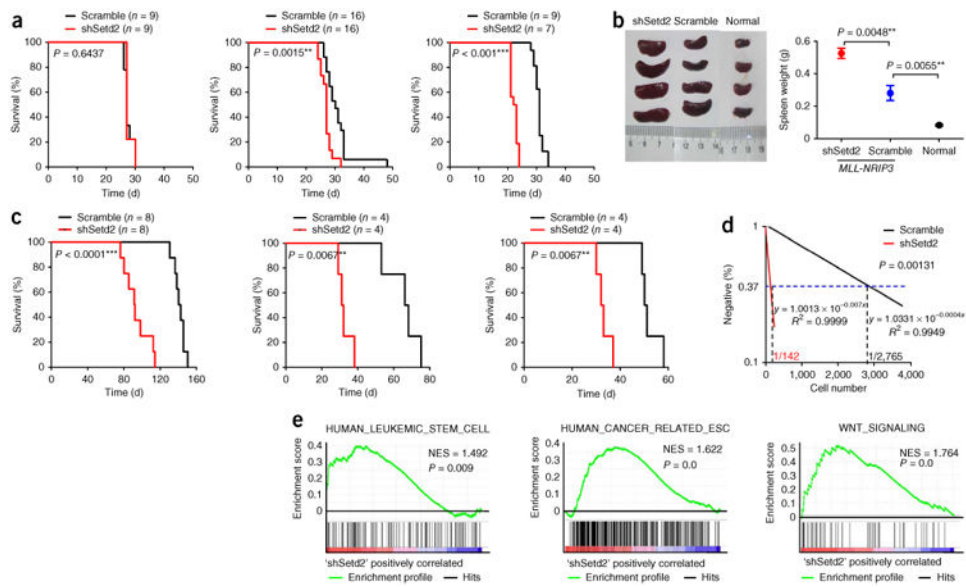
Figure 5.

Functional analysis of *Setd2* in leukemic cells. (**a**) *Setd2* knockdown accelerates *MLL-NRIP3* leukemia in serial BMT assays. *Setd2* knockdown or scrambled shRNA–transduced *MLL-NRIP3* HSPCs were transplanted into recipient mice. For secondary and tertiary BMT, an equal number of *Setd2* knockdown or scrambled shRNA–transduced leukemia cells were transplanted to sublethally irradiated recipient mice. Survival curves of the leukemic mice and the associated *P* values are shown. (**b**) Hepatosplenomegaly in *Setd2* knockdown *MLL-NRIP3* leukemic mice. The spleens themselves (left) and their weights (right; mean ± s.d.; *n* = 4 per group) are shown for *Setd2* knockdown *MLL-NRIP3* leukemic mice, scrambled shRNA–treated *MLL-NRIP3* leukemic mice and normal mice, with the associated *P* values indicated. (**c**) *Setd2* knockdown accelerates *Mll-Af9* leukemia in serial BMT assays. *Setd2* knockdown or scrambled shRNA–transduced *Mll-Af9* knock-in HSPCs were transplanted into recipient mice. For secondary and tertiary BMT, an equal number of *Setd2* knockdown or scrambled shRNA–transduced leukemia cells were transplanted to sublethally irradiated recipient mice. Survival curves of leukemic mice and the associated *P* values are shown. (**d**) Limiting dilution assay. An equal number of *Setd2* knockdown or scrambled shRNA–transduced *Mll-Af9* knock-in leukemia cells isolated from secondary leukemias in cell dosage (as indicated in Supplementary Table 9) were transplanted to sublethally irradiated recipient mice. Leukemia-initiating cell frequencies and the *P* value calculated by L-calc software are shown. (**e**) GSEA[27] plot showing increased gene expression of human leukemia stem cell[28] and cancer-related embryonic stem cell (ESC)[29,30] signatures, as well as Wnt signaling[31,32], in *MLL-NRIP3* leukemia cells with *Setd2* knockdown relative to scrambled shRNA controls. The normalized enrichment score (NES) and *P* values are shown.

Table 1

Major genetic abnormalities identified in *SETD2*-mutated patients with leukemia

Total: 241[a]		Rearranged *MLL*: 27		WT *MLL*: 173	Unknown: 41
Mutated *SETD2*: 15	6 (22.2%[b])	AML: 4[c]	*MLL-NRIP3*: 1[d]	AML: 2	*AML1-ETO*: 1	1
			MLL-AF10: 1[d]		*NPM1* and *CEBPA*: 1[d]	
			Unknown partner: 1			
			MLL-PTD: 1			
		ALL: 2	*MLL-AF9*: 1	ALL: 6	*TEL-AML1*: 1	
			MLL-AF4: 1		*TCR*: 1[d]	
					TCR: 2	
					MDR1: 1	
					Unknown: 1	
WT *SETD2*: 226	21	AML: 14		AML: 77		40
		ALL: 7		ALL: 86		

[a]The number of patients in each leukemia group.

[b]The percentages of patients with *SETD2* mutations in the groups with wild-type (WT) and rearranged *MLL*.

[c]The number of patients with specific genetic mutations.

[d]Biallelic *SETD2* mutation.